

Dynamics of a Discrete Brusselator Model: Escape to Infinity and Julia Set

Hunseok Kang and Yakov Pesin

Abstract. We consider a discrete version of the Brusselator Model of the famous Belousov-Zhabotinsky reaction in chemistry. The original model is a reaction-diffusion equation and its discrete version is a coupled map lattice. We study the dynamics of the local map, which is a smooth map of the plane. We discuss the set of trajectories that escape to infinity as well as analyze the set of bounded trajectories – the Julia set of the system.

Mathematics Subject Classification (2000). Primary 37N25; Secondary 37N10; Tertiary 35K57.

Keywords. Coupled Map Lattices, Brusselator Model, reaction-diffusion equation, Julia set.

1. The Brusselator model for the Belousov-Zhabotinsky reaction

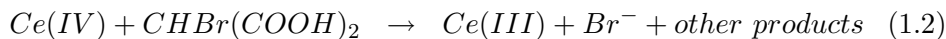
The Brusselator model is a famous model of chemical reactions with oscillations. It was proposed by Prigogine and Lefever in 1968 and the name was coined by Tyson (see [6]). In the middle of the last century Belousov and Zhabotinsky discovered chemical systems exhibiting oscillations. More precisely, they observed that cerium(III) and cerium(IV) were the cycling species: in a mix of potassium bromate, cerium(IV) sulfate, and citric acid in

The work was partially supported by National Science Foundation grant #DMS-0088971 and U.S.-Mexico Collaborative Research grant 0104675

The article is available online on SpringerLink (www.springerlink.com) using colors instead of greyscales in the pictures.

dilute sulfuric acid, the ratio of concentration of the $Ce(IV)$ and $Ce(III)$ ions oscillated. While for most chemical reaction a state of homogeneity and equilibrium is quickly reached, the Belousov-Zhabotinsky reaction is a remarkable chemical reaction that maintains a prolonged state of non-equilibrium leading to macroscopic temporal oscillations and spatial pattern formation that is very life-like.

The simplified mechanism for the Belousov-Zhabotinsky reaction is as follows (see [5]):



Equation (1.1) is autocatalyzed by BrO_3^- , and strongly inhibited by Br^- ions. Therefore, as $Ce(IV)$ is produced in equation (1.1), the rate of equation (1.2) increases. This results in a high concentration of Br^- which inhibits and slows equation (1.1). After the discovery of oscillating chemical reactions, in 1968 Prigogine proposed a virtual oscillating chemical reaction system – the Brusselator model.

The net reaction is $\mathcal{A} + \mathcal{B} \rightarrow \mathcal{D} + \mathcal{E}$ with transient appearance of intermediates \mathcal{X} and \mathcal{Y} . Here \mathcal{A} and \mathcal{B} are reactants and \mathcal{D} and \mathcal{E} are products. The reaction consists of four steps shown on Table 1.1. Step 3 is autocatalytic, since two \mathcal{X} molecules make three \mathcal{X} molecules and it also has an inhibiting factor because, while \mathcal{Y} is necessary to make the reaction, in this process \mathcal{Y} is also used. Indeed, it is the autocatalytic reaction that causes the chemical oscillations in the Brusselator model. On the basis of the Brusselator model, one can create a realistic oscillating chemical reaction model using the Belousov-Zhabotinsky reaction.

To find the equations that govern the Brusselator model denote by A , B , D and E the concentrations of \mathcal{A} , \mathcal{B} , \mathcal{D} and \mathcal{E} , respectively. Assuming that the concentrations A and B are held constant during the chemical reaction and that the system has only one spatial dimension, one obtains the following system of differential equations (by using the column Step Contribution in the Table 1.1 with proper values of coefficients k_i , $i = 1, 2, 3, 4$):

$$\begin{aligned} \frac{\partial u_1}{\partial t} &= A - (B + 1)u_1 + u_1^2 u_2 + \kappa_1 \frac{\partial^2 u_1}{\partial x^2}, \\ \frac{\partial u_2}{\partial t} &= B u_1 - u_1^2 u_2 + \kappa_2 \frac{\partial^2 u_2}{\partial x^2}, \end{aligned} \quad (1.3)$$

Step	Reaction	Step Contribution
1	$\mathcal{A} \rightarrow \mathcal{X}$	$\frac{\partial A}{\partial t} = -k_1 A$ $\frac{\partial u_1}{\partial t} = k_1 A$
2	$\mathcal{B} + \mathcal{X} \rightarrow \mathcal{Y} + \mathcal{D}$	$\frac{\partial B}{\partial t} = -k_2 B u_1$ $\frac{\partial u_1}{\partial t} = -k_2 B u_1$ $\frac{\partial u_2}{\partial t} = k_2 B u_1$ $\frac{\partial D}{\partial t} = k_2 B u_1$
3	$2\mathcal{X} + \mathcal{Y} \rightarrow 3\mathcal{X}$	$\frac{\partial u_1}{\partial t} = -k_3 u_1^2 u_2$ $\frac{\partial u_1}{\partial t} = k_3 u_1^2 u_2$
4	$\mathcal{X} \rightarrow \mathcal{E}$	$\frac{\partial u_1}{\partial t} = -k_4 u_1$ $\frac{\partial E}{\partial t} = k_4 u_1$

TABLE 1.1. Reaction Diagram in the Brusselator model.

where κ_i , $i = 0, 1$ are diffusion constants, x is the spatial coordinate and u_i , $i = 1, 2$ are functions of x and t which represent concentrations of the compounds \mathcal{X} and \mathcal{Y} .

2. A coupled map lattice associated with the Brusselator model

In this paper we are interested in the discrete version of the Brusselator model, which one obtains by discretizing the reaction-diffusion equation (1.3). This is usually the way the equation is studied by a computer. Moreover, for some values of parameters the discrete version itself can be used as an original phenomenological model (see the discussion in [2]).

For the derivative in time we use

$$\frac{\partial u(x, t)}{\partial t} \rightarrow \frac{u(x, t + \Delta t) - u(x, t)}{\Delta t}.$$

And for the space derivative we use

$$\begin{aligned}\frac{\partial u(x, t)}{\partial x} &\rightarrow \frac{u(x + \Delta x, t) - u(x, t)}{\Delta x}, \\ \frac{\partial^2 u(x, t)}{\partial x^2} &\rightarrow \frac{u(x + \Delta x, t) - 2u(x, t) + u(x - \Delta x, t)}{(\Delta x)^2}.\end{aligned}$$

By plugging these discretizations into the system (1.3), we obtain a coupled map lattice (CML) of the type:

$$u_j(n+1) = f(u_j(n)) + \epsilon g_j(\{u_i(n)\}_{|i-j| \leq s}), \quad (2.1)$$

where $n \in \mathbb{Z}$ is the discrete time coordinate and j the discrete space coordinate (see [4]). Furthermore, $f : \mathbb{R}^2 \rightarrow \mathbb{R}^2$ is the *local map* for the CML and is given by

$$f(u_1, u_2) = (a + (1 - \gamma - b)u_1 + \gamma u_1^2 u_2, u_2 + bu_1 - \gamma u_1^2 u_2), \quad (2.2)$$

where $a = A\Delta t > 0$, $b = B\Delta t > 0$ are two leading parameters, and $\gamma = \Delta t > 0$ is a parameter. Finally, $g : (\mathbb{R}^2)^{2s+1} \rightarrow \mathbb{R}^2$ is the *interaction of finite size* s . We assume that ϵ is a sufficiently small parameter by selecting small discretization steps appropriately.

In this paper we study the dynamics of the local map f , mainly describing trajectories that escape to infinity as well as trajectories that remain bounded. The latter form a Cantor-like set in the plane (of apparently positive area) that is the *Julia set* of the system. In this paper we only establish existence of this set and describe a procedure that allows one to construct it. The topological structure of the Julia set is very complicated and is yet to be understood.

As shown in [1, 3] the dynamics of the local map determines the dynamics of the evolution operator for Equation (2.1) on the space of traveling wave solutions. The latter is a finite-dimensional subspace in the infinite-dimensional phase space of the system. Our results in particular, provide a ground for existence of a Julia set for the evolution operator. The detailed discussion of this topic will be given in forthcoming publications.

3. Linear analysis of the local map

We write $f(u_1, u_2) = (f_1(u_1, u_2), f_2(u_1, u_2))$ where

$$\begin{aligned}f_1(u_1, u_2) &= a + (1 - \gamma - b)u_1 + \gamma u_1^2 u_2, \\ f_2(u_1, u_2) &= u_2 + bu_1 - \gamma u_1^2 u_2.\end{aligned}$$

For all values of the parameters $a > 0$, $b > 0$, and $\gamma > 0$ the map f has only one fixed point

$$(v_1, v_2) = \left(\frac{a}{\gamma}, \frac{b}{a}\right). \quad (3.1)$$

We describe stability of the fixed point. The Jacobian matrix is

$$Jac|_{(v_1, v_2)} = \begin{bmatrix} 1 - \gamma + b & \frac{a^2}{\gamma} \\ -b & 1 - \frac{a^2}{\gamma} \end{bmatrix} \quad (3.2)$$

and the characteristic polynomial $p(\lambda)$

$$p(\lambda) = \lambda^2 - (2 - \gamma + b - \frac{a^2}{\gamma})\lambda + (1 - \frac{a^2}{\gamma} - \gamma + a^2 + b). \quad (3.3)$$

The discriminant D of $p(\lambda)$ is

$$D = (\gamma - b)^2 + a^2\left(\frac{a^2}{\gamma^2} - 2 - \frac{2b}{\gamma}\right)$$

and the symmetric axis

$$\lambda_s = \frac{1}{2}\left(2 - \gamma + b - \frac{a^2}{\gamma}\right).$$

Note that $p(1) = a^2 > 0$.

CASE 1. The fixed point is hyperbolic

If $p(-1)$ is negative then, by the intermediate value theorem, there exist two eigenvalues λ_1, λ_2 such that one of them, say λ_1 , is between -1 and 1 , and the other, λ_2 , is less than -1 . Therefore, the fixed point is hyperbolic if

$$p(-1) = \left(1 - \frac{2}{\gamma}\right)a^2 + 2b + 4 - 2\gamma < 0.$$

CASE 2. The fixed point is attracting or repelling

The fixed point is attracting if one of the following sets of conditions holds.

The first one corresponds to real eigenvalues $\lambda_1 \geq \lambda_2$

$$\begin{aligned} D &= (\gamma - b)^2 + a^2\left(\frac{a^2}{\gamma^2} - 2 - \frac{2b}{\gamma}\right) > 0, \\ p(-1) &= \left(1 - \frac{2}{\gamma}\right)a^2 + 2b + 4 - 2\gamma > 0, \\ |\lambda_s| &= \left|\frac{1}{2}\left(2 - \gamma + b - \frac{a^2}{\gamma}\right)\right| < 1, \end{aligned}$$

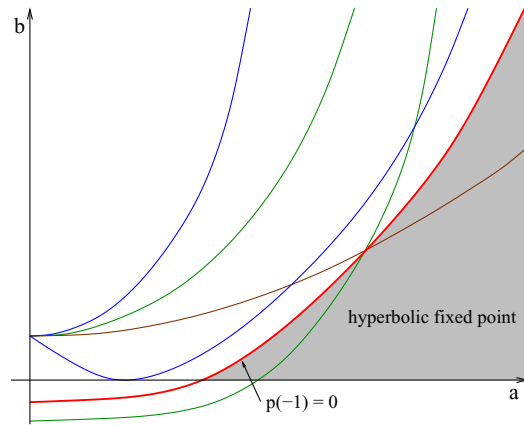


FIGURE 3.1. When $0 < \gamma < 2$, for any parameters $a > 0$ and $b > 0$ in the shaded region, the local map f has a hyperbolic fixed point. The thick curve represents the graph of $p(-1) = 0$ and is a parabola.

and the second one to complex eigenvalues $|\lambda_1| = |\lambda_2|$

$$D = (\gamma - b)^2 + a^2 \left(\frac{a^2}{\gamma^2} - 2 - \frac{2b}{\gamma} \right) < 0,$$

$$|\lambda_1| = \left(1 - \frac{a^2}{\gamma} - \gamma + a^2 + b \right) < 1.$$

Similarly, the fixed point is repelling if one of the following sets of conditions holds. The first one corresponds to real eigenvalues $\lambda_1 \geq \lambda_2$

$$D = (\gamma - b)^2 + a^2 \left(\frac{a^2}{\gamma^2} - 2 - \frac{2b}{\gamma} \right) > 0,$$

$$p(-1) = \left(1 - \frac{2}{\gamma} \right) a^2 + 2b + 4 - 2\gamma > 0,$$

$$|\lambda_s| = \left| \frac{1}{2} \left(2 - \gamma + b - \frac{a^2}{\gamma} \right) \right| > 1,$$

and the second one to complex eigenvalues $|\lambda_1| = |\lambda_2|$

$$D = (\gamma - b)^2 + a^2 \left(\frac{a^2}{\gamma^2} - 2 - \frac{2b}{\gamma} \right) < 0,$$

$$|\lambda_1| = \left(1 - \frac{a^2}{\gamma} - \gamma + a^2 + b \right) > 1.$$

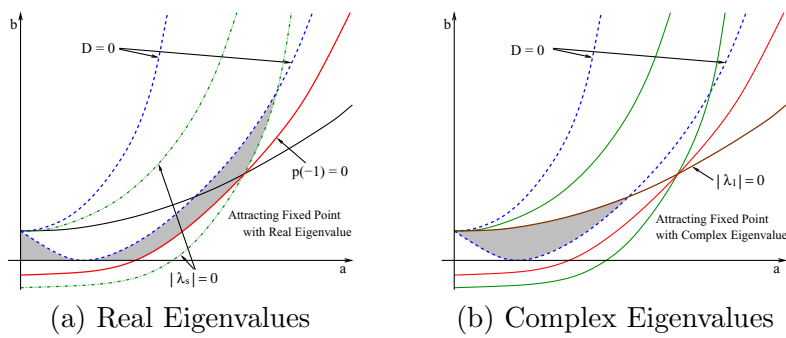


FIGURE 3.2. When $0 < \gamma < 2$, for any parameters $a > 0$, $b > 0$ in the shaded region in (a), the local map f has an attracting fixed point and its Jacobian matrix has real eigenvalues. For those in (b), f also has an attracting fixed point but its Jacobian matrix has complex eigenvalues.

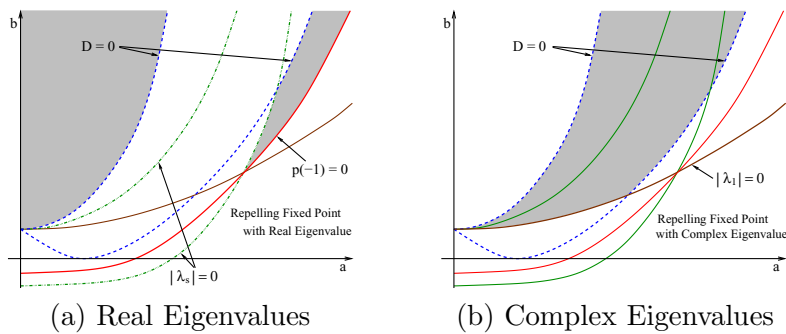


FIGURE 3.3. When $0 < \gamma < 2$, for any parameters $a > 0$, $b > 0$ in the shaded region in (a), the local map f has a repelling fixed point and its Jacobian matrix has real eigenvalues. For those in (b), f also has a repelling fixed point but its Jacobian matrix has complex eigenvalues.

4. Escape to infinity

In this section, we describe a region R in the u_1u_2 -plane such that any trajectory in R escapes to infinity, i.e., $|f^n(u_1, u_2)| \rightarrow \infty$ as $n \rightarrow \infty$. In addition, we will check the behavior of these trajectories in this region.

Lemma 4.1. *For all values of parameters $a > 0$, $b > 0$, and $\gamma > 0$, there exists a region A , that is symmetric with respect to the origin, such that for any point $(u_1, u_2) \in A$,*

$$|f_1(u_1, u_2)| > |u_1| + 2a. \quad (4.1)$$

Proof. Set $m := \max(|2 - \gamma - b|, \gamma + b)$ and define the region A on the plane as follows:

$$A = \{(u_1, u_2) : \gamma u_1^2 |u_2| - m |u_1| - a \geq 0\}.$$

Fix $t > 0$. The following four points lie on the boundary of A in each quadrant:

$$\begin{aligned} (p_{11}, p_{12}) &:= \left(t, \frac{mt + a}{\gamma t^2} \right), \\ (p_{21}, p_{22}) &:= \left(-t, \frac{mt + a}{\gamma t^2} \right), \\ (p_{31}, p_{32}) &:= \left(-t, -\frac{mt + a}{\gamma t^2} \right), \\ (p_{41}, p_{42}) &:= \left(t, -\frac{mt + a}{\gamma t^2} \right). \end{aligned}$$

It is easy to verify that

$$\begin{aligned} f_1(p_{11}, p_{12}) &> 0, & f_1(p_{21}, p_{22}) &> 0, \\ f_1(p_{31}, p_{32}) &< 0, & f_1(p_{41}, p_{42}) &< 0. \end{aligned}$$

We also have that for any $(u_1, u_2) \in \mathbb{R}^2$,

$$\frac{\partial f_1}{\partial u_2}(u_1, u_2) = \gamma u_1^2 \geq 0.$$

Using this one can show

$$f_1(u_1, u_2) > 0 \text{ for any } u_1 \geq p_{11}, u_2 \geq p_{12} \text{ and } u_1 \leq p_{21}, u_2 \geq p_{22},$$

$$f_1(u_1, u_2) < 0 \text{ for any } u_1 \leq p_{31}, u_2 \leq p_{32} \text{ and } u_1 \geq p_{41}, u_2 \leq p_{42}.$$

In the case $u_1 \geq p_{11}$ and $u_2 \geq p_{12}$ this yields

$$\begin{aligned} g_1(u_1, u_2) = |f_1(u_1, u_2)| - |u_1| &= a + (1 - \gamma - b)u_1 + \gamma u_1^2 u_2 - u_1 \\ &= a - (\gamma + b)u_1 + \gamma u_1^2 u_2. \end{aligned}$$

It is easy to see that

$$g_1(p_{11}, p_{12}) = 2a + t(m - \gamma + b) > 2a$$

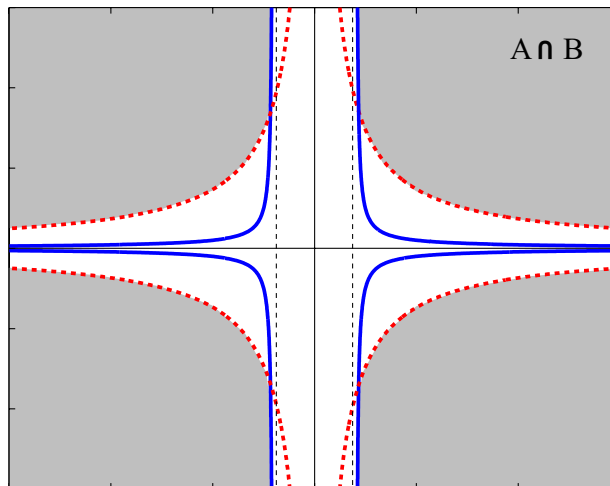


FIGURE 4.1. The shaded area is the intersection $A \cap B$. The solid line is the boundary of B and has two vertical asymptotic lines, $u_1 = -\sqrt{\frac{2}{\gamma}}$ and $u_1 = \sqrt{\frac{2}{\gamma}}$. The dotted line is the boundary of A .

and that

$$\frac{\partial g_1}{\partial u_2}(u_1, u_2) = \gamma u_1^2 \geq 0.$$

Thus, in this case (4.1) holds. Similar calculations show that (4.1) is satisfied in the remaining cases when 1) $u_1 \leq p_{21}$ and $u_2 \geq p_{22}$, 2) $u_1 \leq p_{31}$ and $u_2 \leq p_{32}$, 3) $u_1 \geq p_{41}$ and $u_2 \leq p_{42}$. \square

Lemma 4.1 does not guarantee that for all $n \geq 2$,

$$|f_1(f^{n-1}(u_1, u_2))| > |f_1(f^{n-2}(u_1, u_2))|.$$

Therefore, we introduce another symmetric region B of the plane and so that $R = A \cap B$.

Lemma 4.2. *For all values of parameters $a > 0$, $b > 0$, and $\gamma > 0$, there exists a region B , that is symmetric with respect to the origin, such that for any point $(u_1, u_2) \in B$,*

$$|f_2(u_1, u_2)| > |u_2|. \quad (4.2)$$

Proof. Define the region B as follows:

$$B = \{(u_1, u_2) : |(\gamma u_1^2 - 2)u_2| - b|u_1| \geq 0, \gamma u_1^2 \geq 2\}.$$

Let $s > \sqrt{\frac{2}{\gamma}}$. Then the following four points lie on the boundary of B in each quadrant:

$$\begin{aligned}(q_{11}, q_{12}) &:= \left(s, \frac{bs}{\gamma s^2 - 2} \right), \\(q_{21}, q_{22}) &:= \left(-s, \frac{bs}{\gamma s^2 - 2} \right), \\(q_{31}, q_{32}) &:= \left(-s, -\frac{bs}{\gamma s^2 - 2} \right), \\(q_{41}, q_{42}) &:= \left(s, -\frac{bs}{\gamma s^2 - 2} \right).\end{aligned}$$

It is easy to verify that

$$\begin{aligned}f_2(q_{11}, q_{12}) &< 0, & f_2(q_{21}, q_{22}) &< 0, \\f_2(q_{31}, q_{32}) &> 0, & f_2(q_{41}, q_{42}) &> 0.\end{aligned}$$

We also have that for any $(u_1, u_2) \in \mathbb{R}^2$,

$$\frac{\partial f_2}{\partial u_2}(u_1, u_2) = 1 - \gamma u_1^2 < 0$$

since we require that $|u_1| > \sqrt{\frac{2}{\gamma}}$. It follows that

$$f_2(u_1, u_2) < 0 \text{ for any } u_1 \geq q_{11}, u_2 \geq q_{12} \text{ and } u_1 \leq q_{21}, u_2 \geq q_{22},$$

$$f_2(u_1, u_2) > 0 \text{ for any } u_1 \leq q_{31}, u_2 \leq q_{32} \text{ and } u_1 \geq q_{41}, u_2 \leq q_{42}.$$

In the case $u_1 \geq q_{11}$ and $u_2 \geq q_{12}$ this yields

$$\begin{aligned}g_2(u_1, u_2) = |f_2(u_1, u_2)| - |u_2| &= -u_2 - bu_1 + \gamma u_1^2 u_2 - u_2 \\ &= -2u_2 - bu_1 + \gamma u_1^2 u_2.\end{aligned}$$

It is easy to see that

$$g_2(q_{11}, q_{12}) = 0$$

and that

$$\frac{\partial g_2}{\partial u_2}(u_1, u_2) = -2 + \gamma u_1^2 \geq 0$$

due to the requirement that $|u_1| > \sqrt{\frac{2}{\gamma}}$. Thus, in this case (4.2) holds.

Similar calculations show that (4.2) is satisfied in the remaining cases when 1) $u_1 \leq q_{21}$ and $u_2 \geq q_{22}$, 2) $u_1 \leq q_{31}$ and $u_2 \leq q_{32}$, 3) $u_1 \geq q_{41}$ and $u_2 \leq q_{42}$. \square

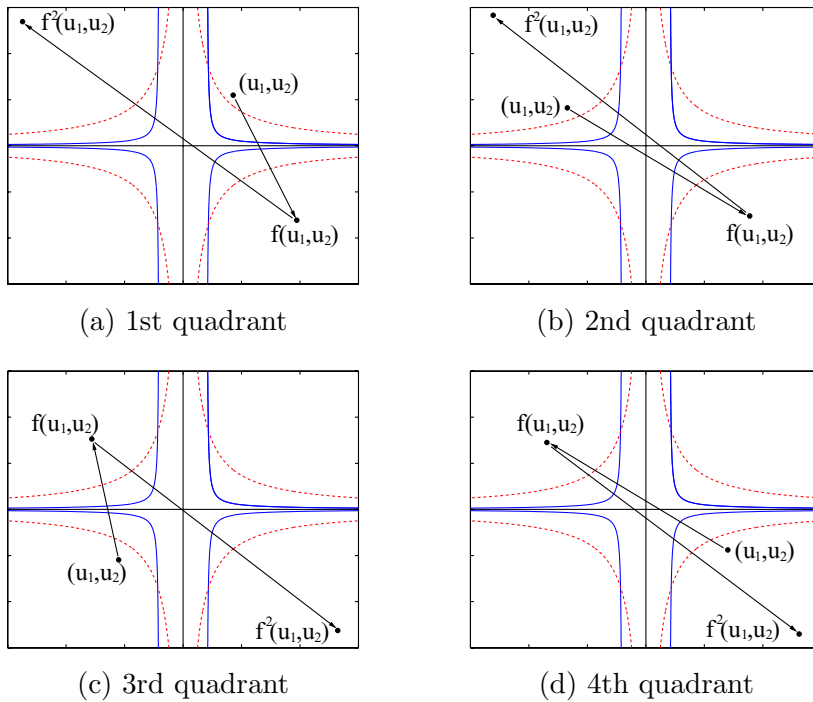


FIGURE 4.2. The way a trajectory escapes to infinity depending on what quadrant it originates in.

Theorem 4.3. *For all values of parameters $a > 0$, $b > 0$, and $\gamma > 0$, there exists a forward-invariant region $R = R(a, b, \gamma)$ such that for any point $(u_1, u_2) \in R$, the trajectory $\{f^n(u_1, u_2)\} \subset R$ escapes to infinity.*

Proof. We claim that $R = A \cap B$ is the desired region. See Figure 4.1. Indeed, by construction of the regions A and B we have for any $(u_1, u_2) \in R$,

$$|f(u_1, u_2)| > |(u_1, u_2)|.$$

Figure 4.2 illustrates various routes of escaping to infinity through the region R depending on what quadrant the original point $(u_1, u_2) \in R$ lies in: from the first and the second quadrant the trajectory moves to the fourth quadrant, from the third quadrant and the fourth quadrant it moves to the second quadrant.

By Lemma 4.1 (see (4.1)), we have that for any $(u_1, u_2) \in R$ with $u_2 > 0$,

$$|f_1(u_1, u_2)| - |u_1| > 2a.$$

In view of Lemma 4.2 (see (4.2)) this implies that

$$|f(u_1, u_2)| - |(u_1, u_2)| > 2a.$$

Observe that any trajectory $\{f^n(u_1, u_2)\}$ that originates in R visits the second quadrant after at most two iterations and hence, we guarantee that for any $(u_1, u_2) \in R$,

$$|f^2(u_1, u_2)| - |(u_1, u_2)| > 2a.$$

This implies that $|f^n(u_1, u_2)| \rightarrow \infty$ as $n \rightarrow \infty$. \square

5. Julia Set of the Local Map

Our goal now is to find the maximal region K so that every point in K escapes to infinity while trajectories of points outside K are bounded. The set $\mathbb{R}^2 \setminus K$ is the Julia set of the system and thus we find various Julia sets corresponding to different values of parameters. We stress that bounded trajectories are the one that are interesting from the physical point of view. We believe that periodic trajectories are dense in the Julia set and that this can be used to justify the existence of oscillating solutions in the Belousov-Zhabotinsky reaction.

In the previous section, we found a region R such that every trajectory originated in R escapes to infinity. In this section we prove that for some values of a , b and γ , every trajectory escaping to infinity gets mapped into R after finitely many iterations of f so that the union of all preimages of R is the desired set K .

Theorem 5.1. *Assume that $a^2 < \gamma$, and $\gamma + b < 1$ and let $\{f^n(u_1, u_2)\}$ be a trajectory that originates in $\mathbb{R}^2 \setminus R$. If this trajectory is unbounded then there exists a positive integer $m = m(a, b, \gamma, u_1, u_2)$ such that $f^m(u_1, u_2) \in R$. In particular, the trajectory escapes to infinity via the region R .*

Proof. Let c_1, c_2 be sufficiently large positive constants and c_3, c_4 sufficiently large negative constants. Define the following four regions of $\mathbb{R}^2 \setminus R$ (see Figure 5.1):

$$\begin{aligned} D_1 &= \{(u_1, u_2) \notin R : u_1 > c_1\}, \\ D_2 &= \{(u_1, u_2) \notin R : u_2 > c_2\}, \\ D_3 &= \{(u_1, u_2) \notin R : u_1 < c_3\}, \\ D_4 &= \{(u_1, u_2) \notin R : u_2 < c_4\}. \end{aligned}$$

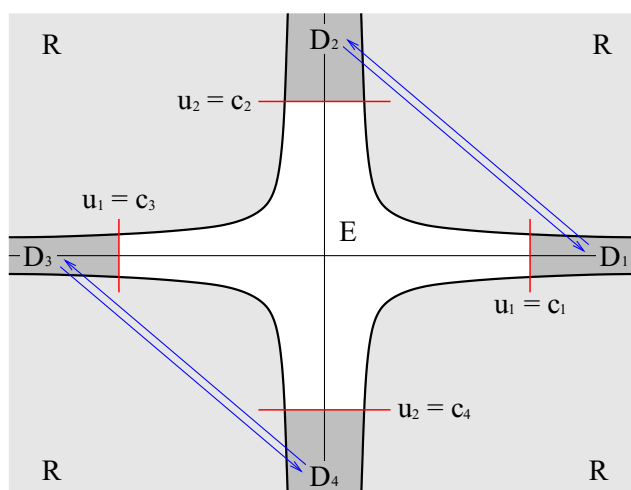


FIGURE 5.1. To the proof of the Theorem 5.1.

Let $D = D_1 \cup D_2 \cup D_3 \cup D_4$ and $E = \mathbb{R}^2 \setminus (R \cup D)$.

We need the following technical lemma.

Lemma 5.2. *For any sufficiently large positive c_1, c_2 , and negative c_3, c_4 , we have*

$$f(u_1, u_2) \notin D_3 \cup D_4,$$

for any $(u_1, u_2) \in D_1 \cup D_2$ and

$$f(u_1, u_2) \notin D_1 \cup D_2,$$

for any $(u_1, u_2) \in D_3 \cup D_4$

This statement allows us to study trajectories that originate in $D_1 \cup D_2$ and $D_3 \cup D_4$ separately. We shall consider only trajectories originating in $D_1 \cup D_2$ as the second case is similar. The following two statements show that no trajectory can stay forever in either of the regions D_1 or D_2 and in particular, escape to infinity via these regions.

Lemma 5.3. *For any sufficiently large $c_1 > 0$ and any $(u_1, u_2) \in D_1$, either $f(u_1, u_2) \notin D_1$ or $f_1(u_1, u_2) < \alpha u_1$ with some $0 < \alpha < 1$.*

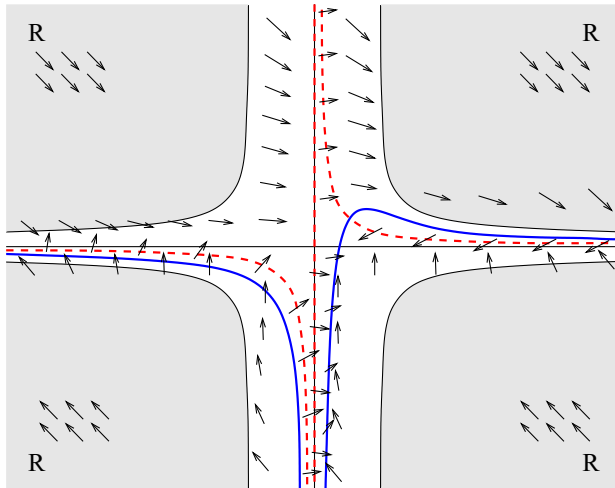


FIGURE 5.2. The directions of trajectories.

Lemma 5.4. *There exists $k \geq 0$ such that for any sufficiently large $c_2 > 0$ and $(u_1, u_2) \in D_2$, the following statements hold:*

1. *for any $(u_1, u_2) \in D_2$, there exists $m = m(u_1, u_2)$ such that $f^m(u_1, u_2) \notin D_2$;*
2. *if $m > 0$ is the first time such that $f^m(u_1, u_2) \notin D_2$ then $f_2(f^i(u_1, u_2)) \leq u_2 + k$ for all $0 \leq i \leq m - 1$.*

The following two statements describe the situation when a trajectory jumps from one of the regions to another.

Lemma 5.5. *For any sufficiently large $c_1 > 0$ and $c_2 > 0$, and any $(u_1, u_2) \in D_1$, let m_1, m_2 be such that $f^i(u_1, u_2) \in D_1$ for $0 \leq i \leq m_1$, $f^j(u_1, u_2) \in D_2$ for $m_1 < j < m_2$, and $f^{m_2}(u_1, u_2) \in D_1$. Then*

$$f_1(f^{m_2-1}(u_1, u_2)) < u_1.$$

Lemma 5.6. *For any sufficiently large $c_1 > 0$ and $c_2 > 0$, and any $(u_1, u_2) \in D_2$, let m_1, m_2 be such that $f^i(u_1, u_2) \in D_2$ for $0 \leq i \leq m_1$, $f^j(u_1, u_2) \in D_1$ for $m_1 < j < m_2$, and $f^{m_2}(u_1, u_2) \in D_2$. Then*

$$f_2(f^{m_2-1}(u_1, u_2)) < u_2 + k,$$

where k is the number in Lemma 5.4.

The proofs of these statements can be obtained by carefully examining the behavior of trajectories originated in each of the sets D_i . Figure 5.2

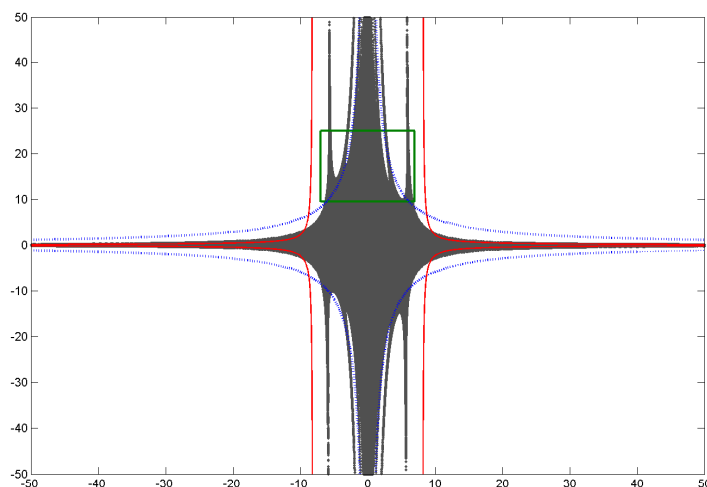


FIGURE 5.3. Julia set for $a = 0.07$, $b = 0.23$, $\gamma = 0.03$, and $N = 20$. The solid line and the dotted line make the boundary of R

shows the directions in the plane along which the trajectories move; the solid curve C_1 and the dotted curve C_2 are given respectively by the equations:

$$\begin{aligned} C_1 &= \{(u_1, u_2) : f_1(u_1, u_2) - u_1 = a - (\gamma + b)u_1 + \gamma u_1^2 u_2 = 0\}, \\ C_2 &= \{(u_1, u_2) : f_2(u_1, u_2) - u_2 = bu_1 - \gamma u_1^2 u_2 = 0\} \end{aligned}$$

and each has two branches. The desired result is an immediate corollary of Lemmas 5.2, 5.3, 5.4, 5.5 and 5.6. \square

Theorem 5.1 provides the following description of the Julia set

$$J = \mathbb{R}^2 \setminus \bigcup_{n \geq 0} f^{-n}(R).$$

The set J is not empty as it contains the fixed point $(v_1, v_2) = (\frac{a}{\gamma}, \frac{b}{a})$ (see Section 3). Figure 5.3 provides a computer generated image of the Julia set and Figure 5.4 shows a magnified piece of the set illustrating its complicated structure. Let us stress that the Julia set is *unbounded* as it contains points in each of D_i with arbitrary large values of u_1 or u_2 respectively. One can show that the Julia set is closed.

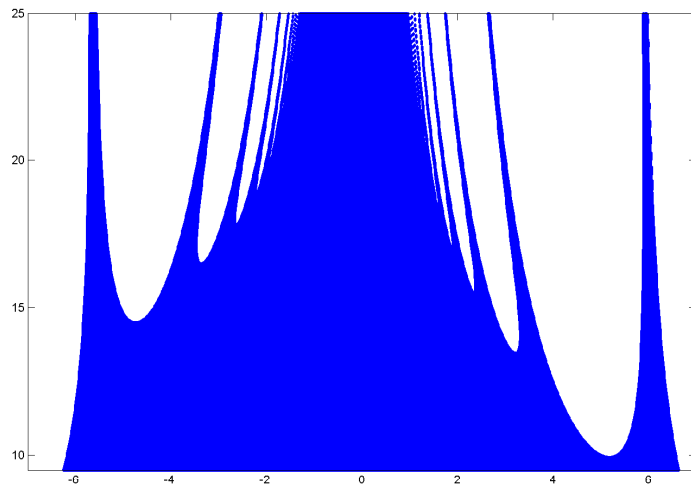


FIGURE 5.4. Zoom-in area of the rectangle in figure 5.3.

To generate images of the Julia set for a sufficiently large $N > 0$ we generate the set of points x for which

$$f^n(x) \in \mathbb{R}^2 \setminus R,$$

for all $n = 0, 1, 2, \dots, N$. One can observe that branches of the Julia set are separated by white regions which are preimages of R . Each branch is further split into more branches and this goes on giving a way to a Cantor-like construction whose limit set is the desired set J .

Here are some interesting questions concerning the topological structure of the Julia set which is very complicated:

1. is J a connected set (as seen on Figure 5.3)?
2. does J have positive area (as seen on Figure 5.3) for all values of parameters?
3. let J_c be the intersection of J with the horizontal line $z = c$; what is the rate of decay of $\text{length}(J_c)$ as $c \rightarrow \infty$?

It is also interesting to describe the dynamics of f on J . In particular,

4. are periodic orbits dense in J ?
5. is the map $f|_J$ hyperbolic for some values of parameters? for example, does it have nonzero Lyapunov exponents for a.e. point with respect to area?

6. does J support any “natural” (in particular, nonatomic) measure invariant under f ?

References

- [1] V. S. Afraimovich and Ya. B. Pesin, *Travelling Waves in Lattice Models of Multi-dimensional and Multi-component Media : I. General Hyperbolic Properties*. Nonlinearity **6** (1993), 429–455.
- [2] K. Kaneko, *Theory and Applications of Coupled Map Lattices*. Wiley, New York, 1993.
- [3] D. R. Orendovici and Ya. B. Pesin, *Chaos in Traveling Waves of Lattice Systems of Unbounded Media*. Springer, IMA Vol. Math. Appl. **119** (2000), 327–358.
- [4] Ya. B. Pesin and A. Yurchenko, *Some Physical Models of The Reaction-Diffusion Equation and Coupled Map Lattices*. Russian Math. Surveys **59**, n.3, vol.8 (2004), 177–218.
- [5] S. H. Strogatz, *Nonlinear Dynamics and Chaos with Applications to Physics, Biology, Chemistry and Engineering*. Studies in Nonlinearity, Addison-Wesley, 1994.
- [6] J. J. Tyson, *The Belousov-Zhabotinskii Reaction*. Lecture Notes in Biomathematics **10**, Springer-Verlag, Heidelberg, 1976.

Hunseok Kang
Department of Mathematics
The Pennsylvania State University
University Park, PA 16802
e-mail: kang@math.psu.edu

Yakov Pesin
Department of Mathematics
The Pennsylvania State University
University Park, PA 16802
e-mail: pesin@math.psu.edu

Lecture held in the *Seminario Matematico e Fisico* on July 1, 2003

Received: March 2005